

## MYELOID NEOPLASIA

## Molecular roulette: nucleophosmin mutations in AML are orchestrated through N-nucleotide addition by TdT

Julian Borrow,<sup>1,2</sup> Sara A. Dyer,<sup>1,2</sup> Susanna Akiki,<sup>1,3</sup> and Michael J. Griffiths<sup>1,2</sup><sup>1</sup>West Midlands Regional Genetics Laboratory, Birmingham Women's and Children's NHS Foundation Trust, Birmingham, United Kingdom; <sup>2</sup>Institute of Cancer and Genomic Studies, University of Birmingham, Birmingham, United Kingdom; and <sup>3</sup>Diagnostic Genomic Division, Department of Laboratory Medicine and Pathology, Hamad Medical Corporation, Doha, Qatar

## KEY POINTS

- *NPM1* mutations in AML arise from replication errors primed by illegitimate TdT activity.
- The involvement of TdT in both *NPM1* and *FLT3-ITD* mutagenesis suggests a significant proportion of AML is a by-product of adaptive immunity.

**Nucleophosmin (*NPM1*) is the most commonly mutated gene in acute myeloid leukemia (AML). AML with mutated *NPM1* is recognized as a separate entity in the World Health Organization 2016 classification and carries a relatively favorable prognosis. *NPM1* mutations are predominantly 4-bp duplications or insertions in the terminal exon that arise through an unknown mechanism. Here we analyze 2430 *NPM1* mutations from 2329 adult and 101 pediatric patients to address their origin. We show that *NPM1* mutations display the hallmarks of replication slippage, but lack suitable germline microhomology available for priming. Insertion mutations display G/C-rich N-nucleotide tracts, with a significant bias toward polypurine and polypyrimidine stacking ( $P < .001$ ). These features suggest terminal deoxynucleotidyl transferase (TdT) primes replication slippage through N-nucleotide addition, with longer syntheses manifesting as N-regions. The recurrent type A, type D, and type B mutations require 1, 2, and 3 N-nucleotide extensions of T, CC, and CAT, respectively, with the last nucleotide used as occult microhomology. This TdT-mutator model**

**successfully predicts the relative incidence of the 256 potential 4-bp insertion/duplication mutations at position c.863\_864 over 4 orders of magnitude ( $\rho = 0.484$ ,  $P < .0001$ ). Children have a different *NPM1* mutation spectrum to adults, including a shift away from type A mutations and toward longer N-regions, consistent with higher TdT activity in pediatric myeloid stem cells. These findings complement our *FLT3-ITD* data, suggesting illegitimate TdT activity contributes to around one-half of AMLs. AML may therefore reflect the price for adaptive immunity. (*Blood*. 2019; 134(25):2291-2303)**

## Introduction

Nucleophosmin (*NPM1*) mutations drive 33% of cases of acute myeloid leukemia (AML), including >50% of cases with a normal karyotype.<sup>1,2</sup> *NPM1*-mutated AML is regarded as a distinct entity in the World Health Organization 2016 classification of myeloid neoplasms<sup>3</sup> on the basis of exclusivity with recurrent cytogenetic rearrangements, CD34 negativity, multilineage involvement, and gene expression profile.<sup>4-8</sup> *NPM1* mutations predict a favorable prognosis unless a *FLT3-ITD* is also present<sup>9,10</sup>; hence, *NPM1* and *FLT3-ITD* mutation status is routinely determined at presentation to facilitate risk-adapted therapy.

*NPM1* is a nucleolar protein that shuttles between nucleus and cytoplasm, contributing to multiple cellular processes.<sup>5,6</sup> In AML, mutated *NPM1* is relocated from the nucleoli to the cytoplasm<sup>2</sup> by creation of a C-terminal leucine-rich nuclear export signal (NES),<sup>11</sup> most commonly of the form L-xxx-V-xx-V-x-L.<sup>5,6</sup> Disruption of the existing nucleolar localization signal through mutation of tryptophans 288 and 290, or just W290, is also

required to create a transforming protein.<sup>6,12,13</sup> Loss of W290 alone necessitates creation of a stronger NES, with substitution of the second hydrophobic position valine with leucine, phenylalanine, cysteine, or methionine (eg, L-xxx-L-xx-V-x-L).<sup>13</sup> Relocation of the mutated protein to the cytoplasm is essential for transformation.<sup>14</sup>

At the DNA level, these changes are achieved through frame-shift of the terminal coding exon. The most common *NPM1* mutation (type A, incidence ~80%)<sup>6</sup> is a 4-bp duplication, c.860\_863dupTCTG,<sup>2</sup> which creates an L-xxx-V-xx-V-x-L NES with loss of both W288 and W290.<sup>5,6</sup> Type B (c.863\_864insCATG) and type D (c.863\_864insCCTG) mutations represent ~10% and ~5% of cases, respectively. All other mutations are considerably rarer,<sup>6</sup> including other 4-bp insertions at c.863\_864, and longer insertions ( $\pm$  deletions) at nearby positions, such as c.869\_873delins(9) which retains W288 and creates a stronger NES.

It is unknown how *NPM1* mutations arise, although a replicative origin is plausible because the most common mutation is a

**Table 1. Adult NPM1 mutation sequences**

Type	Nucleotide sequence of NPM1 mutations	Translation	Occurrence
WT	gatctctggcagtgaggagaagtctctttaa	DLWQWRKSL	NA
	gatct <b>ATGC</b> ctggcagtgaggagaagtctctttaaagaaaatag	DLCLAVEEVSLRK	1
	gatct <b>TTGC</b> ctggcagtgaggagaagtctctttaaagaaaatag	DLCLAVEEVSLRK	1
	gatct <b>TTGTCTG</b> gcagtgaggagaagtctctttaaagaaaatag	DLCLAVEEVSLRK	1
	gatctc <b>ACAA</b> tggcagtgaggagaagtctctttaaagaaaatag	DLTMAVEEVSLRK	1
	gatctc <b>ATTAA</b> gcagtgaggagaagtctctttaaagaaaatag	DLIKAVEEVSLRK	1
	gatctc <b>ATTC</b> tggcagtgaggagaagtctctttaaagaaaatag	DLILAVEEVSLRK	1
	gatctc <b>CGCA</b> tggcagtgaggagaagtctctttaaagaaaatag	DLRMAVEEVSLRK	1
	gatctc <b>GTTTTGGCGA</b> tggaggagaagtctctttaaagaaaatag	DLVLAMEEVSLRK	1
	gatctc <b>TCCATGCTCC</b> tggaggagaagtctctttaaagaaaatag	DLSMLLEEVSLRK	1
	gatctct <b>CCCG</b> gcagtgaggagaagtctctttaaagaaaatag	DLGRAVEEVSLRK	1
	gatctct <b>CTGCAGCCT</b> tggaggagaagtctctttaaagaaaatag	DLSAALEEVSLRK	1
	gatctctg <b>CAAA</b> gcagtgaggagaagtctctttaaagaaaatag	DLCKAVEEVSLRK	1
	gatctctg <b>CAAG</b> gcagtgaggagaagtctctttaaagaaaatag	DLCKAVEEVSLRK	3
	gatctctg <b>CACA</b> gcagtgaggagaagtctctttaaagaaaatag	DLCTAVEEVSLRK	1
	gatctctg <b>CACCACCT</b> tggaggagaagtctctttaaagaaaatag	DLCTTLEEVSLRK	1
	gatctctg <b>CACG</b> gcagtgaggagaagtctctttaaagaaaatag	DLCTAVEEVSLRK	1
	gatctctg <b>CACGCG</b> agtgaggagaagtctctttaaagaaaatag	DLCTRVEEVSLRK	1
	gatctctg <b>CAGA</b> gcagtgaggagaagtctctttaaagaaaatag	DLCRAVEEVSLRK	6
	gatctctg <b>CAGG</b> gcagtgaggagaagtctctttaaagaaaatag	DLCRAVEEVSLRK	7
	gatctctg <b>CAGTAAG</b> gtggaggagaagtctctttaaagaaaatag	DLCSKVEEVSLRK	1
	gatctctg <b>CAGTCG</b> agtgaggagaagtctctttaaagaaaatag	DLCSRVEEVSLRK	1
B	gatctctg <b>CATG</b> gcagtgaggagaagtctctttaaagaaaatag	DLCMAVEEVSLRK	197
	gatctctg <b>CCAC</b> gcagtgaggagaagtctctttaaagaaaatag	DLCHAVEEVSLRK	1
	gatctctg <b>CCAG</b> gcagtgaggagaagtctctttaaagaaaatag	DLCQAVEEVSLRK	11
	gatctctg <b>CCAGAG</b> agtgaggagaagtctctttaaagaaaatag	DLCQRVEEVSLRK	1
	gatctctg <b>CCGA</b> gcagtgaggagaagtctctttaaagaaaatag	DLCRAVEEVSLRK	3
	gatctctg <b>CCGC</b> gcagtgaggagaagtctctttaaagaaaatag	DLCRAVEEVSLRK	1
	gatctctg <b>CCGCCT</b> agtgaggagaagtctctttaaagaaaatag	DLCLRVVEEVSLRK	1
	gatctctg <b>CCGG</b> gcagtgaggagaagtctctttaaagaaaatag	DLCRAVEEVSLRK	11
	gatctctg <b>CCGTT</b> cagtgaggagaagtctctttaaagaaaatag	DLCRSVEEVSLRK	1
D	gatctctg <b>CCTG</b> gcagtgaggagaagtctctttaaagaaaatag	DLCLAVEEVSLRK	160
	gatctctg <b>CGCC</b> gcagtgaggagaagtctctttaaagaaaatag	DLCAAVEEVSLRK	1

Inserted bases are shown in capital letters in the second column. The 4 conserved hydrophobic positions of the nuclear export signal are in bold-face type in the third column. The first base shown is c.856 from the coding reference sequence.

NA, not available.

Table 1. (continued)

Type	Nucleotide sequence of <i>NPM1</i> mutations	Translation	Occurrence
	gatctctg <b>CGTG</b> gcagtggaggaagtctctttaagaaaatag	DLCVAVEEVSLRK	3
	gatctctg <b>CTCG</b> gcagtggaggaagtctctttaagaaaatag	DLCSAVEEVSLRK	4
	gatctctg <b>CTGG</b> gcagtggaggaagtctctttaagaaaatag	DLCWAVEEVSLRK	1
	gatctctg <b>CTTG</b> gcagtggaggaagtctctttaagaaaatag	DLCLAVEEVSLRK	32
	gatctctg <b>TAAA</b> gcagtggaggaagtctctttaagaaaatag	DLCKAVEEVSLRK	1
	gatctctg <b>TAAG</b> gcagtggaggaagtctctttaagaaaatag	DLCKAVEEVSLRK	7
	gatctctg <b>TACCTCC</b> tggaggaagtctctttaagaaaatag	DLCTFLEEVSLRK	1
	gatctctg <b>TACG</b> gcagtggaggaagtctctttaagaaaatag	DLCTAVEEVSLRK	1
	gatctctg <b>TAGC</b> gcagtggaggaagtctctttaagaaaatag	DLCSAVEEVSLRK	1
	gatctctg <b>TAGG</b> gcagtggaggaagtctctttaagaaaatag	DLCRAVEEVSLRK	4
	gatctctg <b>TATG</b> gcagtggaggaagtctctttaagaaaatag	DLCMAVEEVSLRK	18
	gatctctg <b>TCAAGACTTTCTTA</b> aagtctctttaagaaaatag	DLCQDFLKVSLRK	1
	gatctctg <b>TCAG</b> gcagtggaggaagtctctttaagaaaatag	DLCQAVEEVSLRK	9
	gatctctg <b>TCAT</b> gcagtggaggaagtctctttaagaaaatag	DLCHAVEEVSLRK	2
	gatctctg <b>TCGC</b> gcagtggaggaagtctctttaagaaaatag	DLCRAVEEVSLRK	1
	gatctctg <b>TCGG</b> gcagtggaggaagtctctttaagaaaatag	DLCRAVEEVSLRK	8
	gatctctg <b>TCGGAGTCTCGGCGGAC</b> tctctttaagaaaatag	DLCRSLGGLSLRK	1
	gatctctg <b>TCGT</b> gcagtggaggaagtctctttaagaaaatag	DLCRAVEEVSLRK	1
A	gatctctg <b>TCTG</b> gcagtggaggaagtctctttaagaaaatag	DLCLAVEEVSLRK	1750
	gatctctg <b>TGAC</b> gcagtggaggaagtctctttaagaaaatag	DLCDAVEEVSLRK	1
	gatctctg <b>TGCG</b> gcagtggaggaagtctctttaagaaaatag	DLCAAVEEVSLRK	1
	gatctctg <b>TGTG</b> gcagtggaggaagtctctttaagaaaatag	DLCVAVEEVSLRK	2
	gatctctg <b>TTCC</b> gcagtggaggaagtctctttaagaaaatag	DLCSAVEEVSLRK	1
	gatctctg <b>TTCG</b> gcagtggaggaagtctctttaagaaaatag	DLCSAVEEVSLRK	3
	gatctctg <b>TTTG</b> gcagtggaggaagtctctttaagaaaatag	DLCLAVEEVSLRK	2
	gatctctggca <b>AAGGA</b> tggaggaagtctctttaagaaaatag	DLWQRMEEVSLRK	1
	gatctctggca <b>AGATTTCTTAAATC</b> gtctctttaagaaa tagtttaa	DLWQDFLNRLFVK IV	1
	gatctctggcag <b>AAGT</b> tggaggaagtctctttaagaaaatag	DLWQKLEEVSLRK	1
	gatctctggcag <b>AGAA</b> tggaggaagtctctttaagaaaatag	DLWQRMEEVSLRK	3
	gatctctggcag <b>AGAC</b> tggaggaagtctctttaagaaaatag	DLWQRLEEVSLRK	2
	gatctctggcag <b>AGAT</b> tggaggaagtctctttaagaaaatag	DLWQRLEEVSLRK	1
	gatctctggcag <b>AGGA</b> tggaggaagtctctttaagaaaatag	DLWQRMEEVSLRK	8
	gatctctggcag <b>AGGC</b> tggaggaagtctctttaagaaaatag	DLWQRLEEVSLRK	2

Inserted bases are shown in capital letters in the second column. The 4 conserved hydrophobic positions of the nuclear export signal are in bold-face type in the third column. The first base shown is c.856 from the coding reference sequence.

NA, not available.

Table 1. (continued)

Type	Nucleotide sequence of <i>NPM1</i> mutations	Translation	Occurrence
	gatctctggcag <b>CGCCTT</b> gaggaagtctctttaagaaaatag	DLWQRLEEVSLRK	1
	gatctctggcag <b>CGCT</b> tggaggaagtctctttaagaaaatag	DLWQRLEEVSLRK	1
	gatctctggcag <b>CGGA</b> tggaggaagtctctttaagaaaatag	DLWQRMEEVSLRK	1
	gatctctggcag <b>CGGATGGC</b> ggaagtctctttaagaaaatag	DLWQRMAEVSLRK	1
	gatctctggcag <b>CGGC</b> tggaggaagtctctttaagaaaatag	DLWQRLEEVSLRK	1
	gatctctggcag <b>CGTCTGGCC</b> aagtctctttaagaaaatag	DLWQR LGQVSLRK	1
	gatctctggcag <b>CGTTTC</b> aggaagtctctttaagaaaatag	DLWQR FQEVSLRK	1
	gatctctggcag <b>GGGATAGCGATGC</b> tctctttaagaaaatag	DLWQGIAMLSLRK	1
	gatctctggcag <b>GGGGTGGGGAATC</b> tctctttaagaaaatag	DLWQGVGNLSLRK	1
	gatctctggcagt <b>CCAT</b> ggaggaagtctctttaagaaaatag	DLWQSMEEVSLRK	1
	gatctctggcagt <b>CCTAGCCC</b> aagtctctttaagaaaatag	DLWQSLAQVSLRK	1
	gatctctggcagt <b>CCCTCTCC</b> aagtctctttaagaaaatag	DLWQSLSQVSLRK	1
	gatctctggcagt <b>CCCTGGAGA</b> aagtctctttaagaaaatag	DLWQSLKQVSLRK	1
	gatctctggcagt <b>CCCTTTCCA</b> aagtctctttaagaaaatag	DLWQSLSKVSLRK	1
	gatctctggcagt <b>CCTTTCTA</b> aagtctctttaagaaaatag	DLWQSLSKVSLRK	1
	gatctctggcagt <b>CTCTGGCC</b> aagtctctttaagaaaatag	DLWQSLAQVSLRK	1
	gatctctggcagt <b>CTCTTTCTA</b> aagtctctttaagaaaatag	DLWQSLSKVSLRK	1
	gatctctggcagt <b>CTTTGCTCAC</b> gtctctttaagaaaatag	DLWQSFQVSLRK	1
	gatctctggcagt <b>TATTTTCCC</b> aagtctctttaagaaaatag	DLWQLFSQVSLRK	1
	gatctctggcagt <b>CCTCGAGA</b> aagtctctttaagaaaatag	DLWQCLEKVSLRK	1
	gatctctggcagt <b>CTGCTCCC</b> aagtctctttaagaaaatag	DLWQCCSQVSLRK	1
	gatctctggcagt <b>TTTCTCCC</b> aagtctctttaagaaaatag	DLWQCFQVSLRK	1
	gatctctggcagt <b>TTTTGCTC</b> aagtctctttaagaaaatag	DLWQCFQVSLRK	1
	gatctctggcagt <b>TTTTTCCC</b> aagtctctttaagaaaatag	DLWQCFQVSLRK	2
	gatctctg <b>CAGGCT</b> agtggaggaagtctctttaagaaaatag	DLCR LVEEVSLRK	Rare
	gatctctg <b>CCGCGG</b> agtggaggaagtctctttaagaaaatag	DLCR GVEEVSLRK	Rare
	gatctctg <b>TAGGAAG</b> gtggaggaagtctctttaagaaaatag	DLCR KVEEVSLRK	Rare
	gatctctggca <b>AAGAA</b> tggaggaagtctctttaagaaaatag	DLWQRMEEVSLRK	Rare
	gatctctggca <b>CCGTTTCTCC</b> gaagtctctttaagaaaatag	DLWHRFSEVSLRK	Rare
	gatctctggcag <b>ACTTTCTATA</b> aagtctctttaagaaaatag	DLWQTFYKQVSLRK	Rare
	gatctctggcagt <b>CTTCTCCA</b> aagtctctttaagaaaatag	DLWQCFQVSLRK	Rare

Inserted bases are shown in capital letters in the second column. The 4 conserved hydrophobic positions of the nuclear export signal are in bold-face type in the third column. The first base shown is c.856 from the coding reference sequence.

NA, not available.

duplication.<sup>15</sup> However, there is a significant difference in the incidence of type A mutations between children and adults, potentially suggesting different pathological mechanisms.<sup>5,6,16,17</sup>

Any model should account for this difference. In our accompanying paper, we propose a replication-based model to explain the genesis of *FLT3*-ITDs in which terminal deoxynucleotidyl

transferase (TdT) synthesizes the microhomology for priming replication slippage when germline microhomology is unavailable, with longer syntheses manifesting as G/C-rich N-regions at the repeat junction.<sup>18</sup> The marked cooccurrence of *NPM1* and *FLT3*-ITD mutations suggested to us that TdT could also prime *NPM1* mutations (although these mutations are also known to synergize<sup>19</sup>).

Here we analyze 2430 *NPM1* mutations to explore their genesis. *NPM1* mutations show anatomy consistent with TdT-primed replication slippage, including G/C-rich N-regions with polypurine/polypyrimidine base stacking. Modeling with TdT predicts the frequency of all 256 different 4-bp insertions at c.863\_864, and explains the different *NPM1* mutational spectra observed in children and adults. These observations strengthen the evidence that TdT causes leukemia.

## Materials and methods

### Mutation identification

*NPM1* mutation sequences were identified from papers published up to 2016 via PubMed (supplemental Table 1, available on the *Blood* Web site). Duplicate publications were excluded. The *NPM1* reference sequence was LRG\_458t1, numbering from the start of the coding region.

### *NPM1* mutation dinucleotide analysis

Dinucleotides were identified from *NPM1* N-regions  $\geq 2$  nt. All insertion positions were considered. Each individual mutation was only included once irrespective of incidence.

### Incidence calculations

The predicted incidence of each *NPM1* 4-bp c.863\_864 insertion was calculated using the incidences of the 16 TdT-synthesized dinucleotides and the proportion of each TdT extension length, as determined from *FLT3*-ITD N-regions (supplemental Table 2), and corrected for the percentage of 1-5 nucleotide extensions from c.863 predicted to yield a transforming protein (6.7%). Probabilities were summed for each extension length through which a mutation could occur, excluding nucleotide extensions  $\geq 6$  nt.

### Bioinformatics and statistics

Human codon usage was obtained from <http://www.kazusa.or.jp/codon/>. Cumulative binomial probabilities were calculated at <http://vassarstats.net/binomialX.html>. Fisher's exact tests were performed at <http://www.graphpad.com/quickcalcs/contingency1/>. *P* values are 2-tailed. Spearman's rank correlations were performed at [http://www.wessa.net/rwasp\\_spearman.wasp/](http://www.wessa.net/rwasp_spearman.wasp/).

## Results

### *NPM1* mutation anatomy and priming

The position, sequence, and incidence of 2423 *NPM1* mutations (2322 adults, 101 children) was compiled (Tables 1 and 2). Seven additional unique adult *NPM1* mutations of unknown incidence were appended (Table 1). We identified 114 unique mutations, predominantly short frameshift duplications, insertions,

or indels that impaired the nucleolar localization signal and created an NES.

The most common mutation was the duplication type A c.860\_863dupTCTG (1793/2423, 74.0%), followed by type B c.863\_864insCATG (8.9%) and type D c.863\_864insCCTG (6.9%) insertions. Neither type B or D mutations meet the HGVS definition of a duplication, but both show duplicated bases separated by nucleotides of unknown origin. The 4 additional bases in a type B mutation consist of 2 bases of unknown origin (CA), followed by a 2-bp duplication (TG), whereas type D mutations contain 1 base of unknown origin (C), followed by a 3-bp duplication (CTG). We further identified 1 additional exact duplication, c.871\_872dupTGGA; 142 non-B/non-D duplications with filler; 51 insertions without any duplicated bases; 51 indels; and 2 multiple clustered point mutations that created an NES in the existing ORF. Anatomically, *NPM1* mutations therefore resemble miniature *FLT3*-ITDs, with similar use of junctional filler nucleotides.

Because *NPM1* mutation anatomy was consistent with replication slippage, we sought the germline microhomology anticipated for priming, especially for the highly recurrent type A c.860\_863dupTCTG duplication. Critically, there was no G at c.859 or T at c.864 and hence no germline microhomology available to prime type A duplications. Although duplications can occasionally be generated by nonhomologous end-joining,<sup>20,21</sup> the latter is unlikely to cause a single highly recurrent mutation. There was no evidence of a secondary structure within the breakpoint region.

We also considered whether germline microhomology was available at any other position within the *NPM1* insertion region to prime a 4-bp duplication that could lead to a transforming protein. Such mutations might be predicted at high frequency by a replication-based model. The targeted region of *NPM1* is smaller than that of *FLT3*, with start and end points spread over 16 bp (c.860 to c.876) (Tables 1 and 2). The start region was just 12 bp (c.860 to c.871), with highly uneven use of positions within this region (Table 3). The products of all 12 hypothetical duplications across the start region were assessed (supplemental Table 3). Six of 12 duplications showed germline microhomology, by definition forming 3 identical pairs. Two of these mutations, c.862\_865dupTGGC and c.864\_867dupGCAG, break the W288 rule, retaining p.Trp288 with a weak L-xxx-V-xx-V-x-L type NES,<sup>13</sup> and are likely benign. The third encodes a product not observed in AML. This suggests no germline microhomology is available to prime relevant slippage within the insertion region. We therefore considered whether TdT provides occult microhomology for priming and the filler nucleotides observed in 627/2423 (25.9%) of *NPM1* mutations represented N-nucleotides.

### Characterization of *NPM1* fillers

TdT is biased toward addition of G/C nucleotides, resulting in N-nucleotide G/C content  $\geq 57\%$  in antigen receptors.<sup>22,23</sup> The G/C content of 1614 *NPM1* filler nucleotides was elevated for both adults (57.1%) and children (59.3%) and across all insertion positions (supplemental Table 3). In contrast, flanking genomic DNA of 50 bp to 2 kb, the *NPM1* coding sequence and the human genome have G/C content of 30% to 42%. The G/C content of *NPM1* filler nucleotides is therefore consistent

**Table 2. Pediatric *NPM1* Mutation Sequences**

Type	Nucleotide sequence of <i>NPM1</i> mutations	Translation	Occurrence
WT	gatctctggcagtgagggaagtctctttaa	DLWQWRKSL	NA
	gatctct <b>ATCT</b> ggcagtgagggaagtctctttaaagaaaatag	DLYLAVEEVSLRK	1
	gatctctg <b>CAGG</b> ggcagtgagggaagtctctttaaagaaaatag	DLCRAVEEVSLRK	1
B	gatctctg <b>CATG</b> ggcagtgagggaagtctctttaaagaaaatag	DLCMAVEEVSLRK	18
	gatctctg <b>CCGG</b> ggcagtgagggaagtctctttaaagaaaatag	DLCRAVEEVSLRK	3
D	gatctctg <b>CCTG</b> ggcagtgagggaagtctctttaaagaaaatag	DLCLAVEEVSLRK	8
	gatctctg <b>CGGA</b> ggcagtgagggaagtctctttaaagaaaatag	DLCGAVEEVSLRK	1
	gatctctg <b>CTTG</b> ggcagtgagggaagtctctttaaagaaaatag	DLCLAVEEVSLRK	1
	gatctctg <b>TACG</b> ggcagtgagggaagtctctttaaagaaaatag	DLCTAVEEVSLRK	1
	gatctctg <b>TATG</b> ggcagtgagggaagtctctttaaagaaaatag	DLCMAVEEVSLRK	1
	gatctctg <b>TCAG</b> ggcagtgagggaagtctctttaaagaaaatag	DLCOAVEEVSLRK	1
	gatctctg <b>TCGG</b> ggcagtgagggaagtctctttaaagaaaatag	DLCRAVEEVSLRK	1
A	gatctctg <b>TCTG</b> ggcagtgagggaagtctctttaaagaaaatag	DLCLAVEEVSLRK	43
	gatctctg <b>TGCC</b> ggcagtgagggaagtctctttaaagaaaatag	DLCAAVEEVSLRK	1
	gatctctg <b>TGTG</b> ggcagtgagggaagtctctttaaagaaaatag	DLCVAVEEVSLRK	2
	gatctctggc <b>TCCGATTGC</b> ggaagtctctttaaagaaaatag	DLWLRFAEVSLRK	1
	gatctctggca <b>AGATCTCAGCAAG</b> gtctctttaaagaaaatag	DLWQDLSKVSLRK	1
	gatctctggcag <b>CGGA</b> tggagggaagtctctttaaagaaaatag	DLWQRMEEVSLRK	1
	gatctctggcag <b>CGGATGGCC</b> gaagtctctttaaagaaaatag	DLWQRMMAEVSLRK	1
	gatctctggcag <b>CGGATTCC</b> ggaagtctctttaaagaaaatag	DLWQRPEVSLRK	2
	gatctctggcag <b>CGTTC</b> ggagggaagtctctttaaagaaaatag	DLWQRSEEVSLRK	1
	gatctctggcag <b>ATCTGGGGGCC</b> ggagggaagtctctttaa	DLWQYLGARRKSL	1
	gatctctggcag <b>CCCTCGCCC</b> aagtctctttaaagaaaatag	DLWQSLAQVSLRK	1
	gatctctggcag <b>CCTTTCCC</b> aagtctctttaaagaaaatag	DLWQSFQVSLRK	1
	gatctctggcag <b>GCTTCGCCA</b> aagtctctttaaagaaaatag	DLWQCFQVSLRK	1
	gatctctggcag <b>GTTTTCAA</b> aagtctctttaaagaaaatag	DLWQCFQVSLRK	1
	gatctctggcag <b>TACTTTCCC</b> aagtctctttaaagaaaatag	DLWQLLSQVSLRK	1
	gatctctggcag <b>TATTTCCC</b> aagtctctttaaagaaaatag	DLWQLFSQVSLRK	1
	gatctctggcag <b>CCCT</b> ggaagtctctttaaagaaaatag	DLWQWTLVSLRK	1
	gatctctggcag <b>TGGA</b> ggaagtctctttaaagaaaatag	DLWQWMEVSLRK	1
	gatTtTggcagGggagggaagTtTttaaagaaaatag	DFWQGRKFF	1
	gatctctggcagGggagggaagCctctttaaagaaaatag	DLWQGRKPL	1

Inserted bases are shown in bold capital letters in the second column. The 4 conserved hydrophobic positions of the nuclear export signal are in bold-face type in the third column. The first base shown is c.856 from the coding reference sequence.

**Table 3. Incidence of use of *NPM1* insertion positions**

<i>NPM1</i> Insertion Site	Adult		Pediatric		Adult + pediatric		P
	<i>NPM1</i> mutations, n	<i>NPM1</i> mutations, %	<i>NPM1</i> mutations, n	<i>NPM1</i> mutations, %	<i>NPM1</i> mutations, n	<i>NPM1</i> mutations, %	Adult vs pediatric
860_861	3	0.13	0	0.00	3	0.13	N/T
861_862	6	0.26	0	0.00	6	0.25	N/T
862_863	2	0.09	1	1.01	3	0.13	N/T
863_864	2267	97.63	82	82.83	2349	97.03	<.001
864_865	0	0.00	0	0.00	0	0.00	N/T
865_866	0	0.00	1	1.01	1	0.04	N/T
866_867	2	0.09	1	1.01	3	0.1	N/T
867_868	26	1.12	5	5.05	31	1.28	.008
868_869	10	0.43	7	7.07	17	0.70	<.001
869_870	6	0.26	0	0.00	6	0.25	N/T
870_871	0	0.00	0	0.00	0	0.00	N/T
871_872	0	0.00	2	2.02	2	0.08	N/T
	n = 2322		n = 99		n = 2421		

A Bonferroni correction of 3 was applied, hence a  $P < .0167$  was considered significant. Mutations at positions c.860\_861, c.861\_862 and c.862\_863 may result from loss of 1 to 3 nt from c.863\_864.

N/T, not tested.

with synthesis by TdT. In comparison, junction sequences from *BCOR*-ITDs (short driver duplications found in various solid tumors that lack TdT) did not reveal equivalent G/C rich insertions (J.B., unpublished data 10 August 2019).

*N*-regions from antigen receptors have a mean length of 2.8 to 4.2 nt (range, 1-13),<sup>22,23</sup> whereas *N*-regions from nonantigen receptor loci are more variable (*BTG1*, mean 5.8 nt, range, 1-21<sup>24</sup>; *FLT3*-ITDs, mean 5.6 nt, range, 1-36<sup>18</sup>). The mean length of 627 *NPM1* fillers was 2.6 nt, range, 1-17; only 2/627 fillers exceeded 13 nt in length (supplemental Figure 1). *NPM1* fillers increased in length while decreasing in frequency, but also showed evidence of bimodality, with a major peak at 2 nt and a minor peak at 9 nt. The 9-nt peak reflects indels at c.868\_869 (9-bp insertion; 5-bp deletion). These longer indels may be required to optimize the NES. Overall, the size and range of *NPM1* fillers were consistent with *N*-regions.

A further hallmark of *N*-regions is runs of homopurines and homopyrimidines caused by nucleotide stacking in the absence of template.<sup>25</sup> We analyzed *NPM1* fillers for overrepresentation of purine–purine and pyrimidine–pyrimidine (YY) dinucleotides and underrepresentation of RY and YR dinucleotides. The adult dataset contained 452 dinucleotides from 94 mutations; 7 of 8 purine–purine and YY dinucleotides were overrepresented, 3 significantly, whereas 7 of 8 of the RY and YR dinucleotides were underrepresented, 3 significantly (Table 4). Analyses of pediatric (supplemental Table 4) and combined *NPM1* and *FLT3*-ITD dinucleotide datasets (supplemental Table 5) afforded similar conclusions. These data strongly suggest TdT synthesizes *NPM1* fillers.

### Model for *NPM1* mutation genesis

The data here suggest a model of replication slippage comparable to *FLT3*-ITD genesis,<sup>18</sup> but without use of germline microhomology. To create a type A duplication, TdT would add a T to c.863, allowing illegitimate alignment with position 860. Polymerization from here leads to the TCTG duplication (Figure 1A). Because the T is used for priming, no *N*-nucleotides are visible in the final mutation. To create a type D c.863\_864insCCTG, TdT adds 2 nucleotides, CC. The second of these bases primes from 861, leaving the first C visible as an *N*-nucleotide at the center of a 3-bp interrupted duplication (Figure 1B). Type B mutations occur through addition of 3 nucleotides (CAT) at 863\_864, with the 3' T priming from 862, leaving the CA visible as an *N*-region within a 2-bp interrupted duplication (Figure 1C). To create a 4-bp insertion, TdT adds 5 nt, with the fifth nucleotide used for priming (Figure 1D). Addition of >5 nt by TdT will lead to indel formation through reintegration at positions progressing toward position 877. The longest *N*-region was a 17-nt TCGGAGTCTCGGCGGAC synthesis associated with a 13-bp deletion.

### Incidence prediction of 4-bp insertions at c.863\_864

This model implicitly predicts the relative incidence of all insertions at a given site, assuming no bias against particular translation products. For example, there are 256 (44) different 4-bp sequences that could be inserted at c.863\_864; their relative incidence is predetermined by TdT's G/C bias, nucleotide stacking, and preference for shorter syntheses. These parameters are known for *FLT3*-ITDs, where there is no apparent



**Table 4. Dinucleotide analysis of N-nucleotides from adult *NPM1* mutations**

Dinucleotide	No. obs	No. exp	Obs/exp ratio	P	Significant at P = .05
<b>RR*</b>					
GG	24	17.01	1.41	.065	No
AA	19	16.66	1.14	.318	No
GA	25	16.84	1.48	.032	Yes
AG	28	16.84	1.66	.006	Yes
<b>YY*</b>					
CC	54	55.69	0.97	.612	No
TT	47	31.26	1.50	.004	Yes
CT	42	41.73	1.01	.497	No
TC	44	41.73	1.05	.370	No
<b>RY†</b>					
GC	30	30.78	0.97	.493	No
GT	12	23.06	0.52	.008	Yes
AT	14	22.82	0.61	.034	Yes
AC	15	30.46	0.49	.001	Yes
<b>YR†</b>					
CG	32	30.78	1.04	.638	No
CA	28	30.46	0.92	.378	No
TG	19	23.06	0.82	.228	No
TA	19	22.82	0.83	.258	No

Calculated using frequencies of individual nucleotides G = 0.194, A = 0.192, T = 0.263, and C = 0.351.

\*For the RR and YY dinucleotides, the P value reflects the cumulative binomial probability of the observed value exceeding or equalling the expected value.

†For RY and YR dinucleotides, the P value is for observed values less than or equal to the expected value.

restriction on N-region length or codon usage (supplemental Table 2). Comparison of the predicted and observed incidences for the 256 theoretical c.863\_864 4-bp insertion/duplication mutations (n = 2257 adult mutations) (supplemental Table 6) showed a significant correlation ( $\rho = 0.484$ ,  $P < .0001$ ; Spearman rank correlation) (Figure 2). These results provide strong support for the TdT/occult microhomology model. Aspects of this model are explored in the following section.

The 4-bp insertions at c.863\_864 encode the last base of codon 288 and the entire new codon 289; germline W288 (tryptophan) is encoded by TGG, hence synthesis of N-nucleotides initiates after the TG (Figure 1A). *FLT3*-ITD data suggest TdT adds just a single nucleotide 54.2% of the time. Creation of a functional *NPM1* mutation is a molecular roulette. The probabilities of TdT adding a G, A, T, or C following a G are 0.58, 0.21, 0.09, and 0.12, respectively (values from *FLT3*-ITD N-regions; supplemental Table 2). If chance favors G, priming cannot occur from the required position to create a 4-bp insertion. The lesion might be repaired by reintegration elsewhere, but is unlikely to promote AML. Should TdT add additional nucleotide(s) that do permit priming of a comparable 4-bp frameshift, then the original codon 288 would be recreated to encode tryptophan; the resulting NES would break the W288 rule and fail to transform. None of the 64 4-bp insertions starting with a G were observed. Alternatively, if TdT adds an A as the first nucleotide after c.863, followed by further nucleotide(s) to allow reintegration in the appropriate frame, a TGA stop codon is created. The absence of all 64

4-bp insertions starting with A shows truncated *NPM1* is not transforming. The pool of potential mutations is therefore reduced to 128. In contrast, although addition of a C alone does not permit correct priming for c.863\_864ins(4) mutations, chain elongation will permit integration that can create a leukemogenic mutant.

However, if a T is added after c.863, a type A mutation can be formed through mispriming from nucleotide 860, as shown (Figure 1A). The likelihood of this is obtained by multiplying the frequency of obtaining a single base TdT extension (0.542) by the incidence of a G to T extension by TdT (0.09; supplemental Table 2; derived from *FLT3* N-region data). To obtain the expected incidence, this value must be corrected to reflect events that do not result in a functional protein, either because they result in a stop or lack the correct occult microhomology for priming in the required frame; only 6.7% of all 1 through 5 nucleotide extensions from c.863 yield a potentially functional protein. We must further allow for the additional ways this mutation can occur: 2 through 5 nucleotide extensions of TC, TCT, TCTG, and TCTGG. Summing these probabilities shows the expected incidence of a type A mutation is 79.6%. Among 2257 mutations, we would therefore expect 1797 type A mutations; 1750 were observed.

As expected, only mutations starting with T or C were observed. The number of possible mutations can be further reduced by 6 to reflect the 3 stop codons preceded by T or C; the total number of mutations considered possible was therefore 122. The rarest predicted mutations were c.863\_844insCGCT and



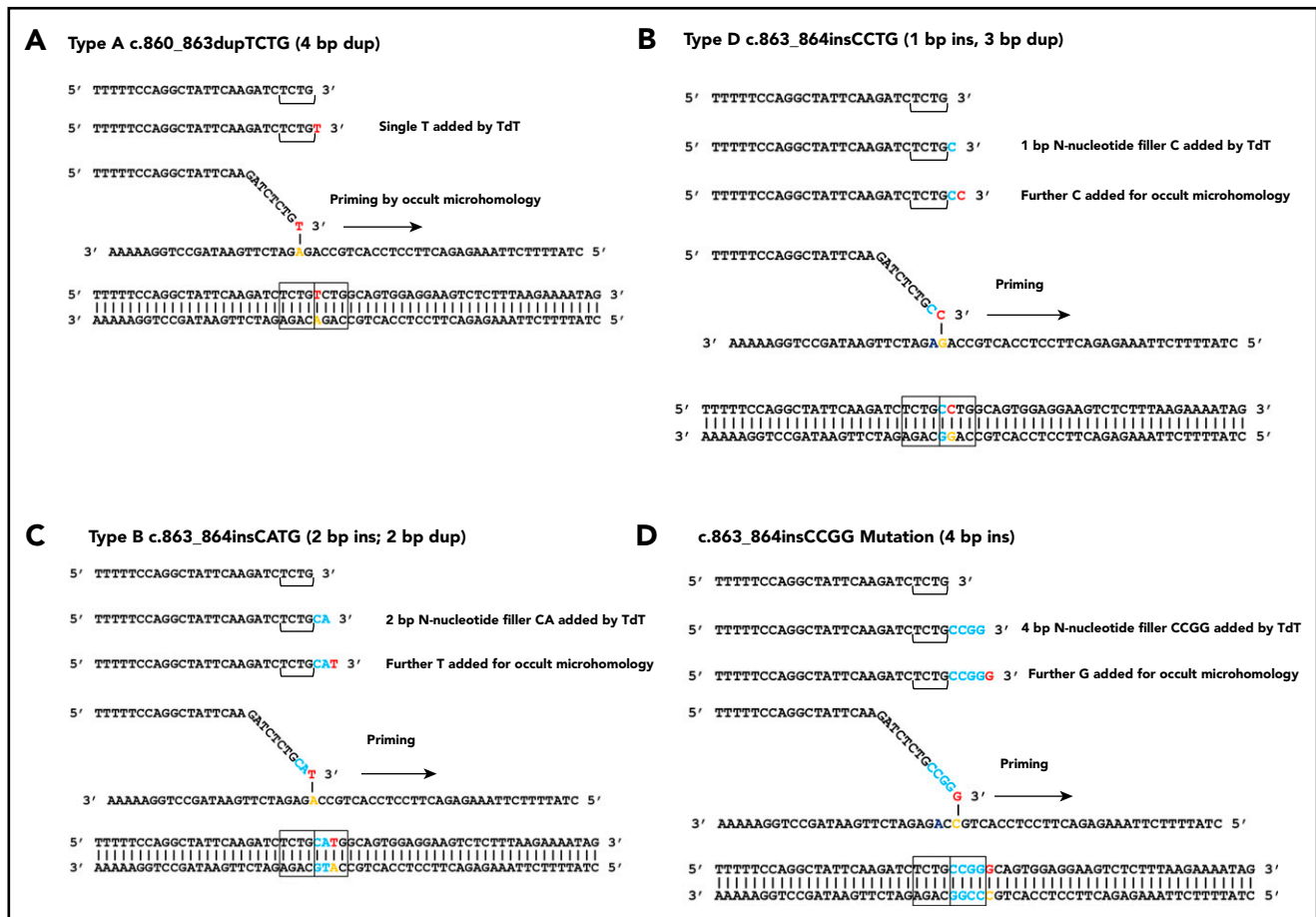


**Figure 1. TdT/ocult microhomology model for genesis of *NPM1* mutations.** (A) Type A mutation, single base of occult microhomology. (B) Type D mutation, 2 nucleotides added, the first visible as an N-nucleotide, the second used for occult microhomology. (C) Type B mutation, 3 nucleotides added, 2 visible as N-nucleotides. (D) c.863\_864insCCGG mutation, 5 nucleotides added, 4 visible as N-nucleotides.

c.863\_844insCTGC (expected incidence <0.001%) (supplemental Table 6). To create these mutations, TdT must add 5 N-nucleotides, with the fifth nucleotide, G, providing occult microhomology; such extensions provide many permutations. The incidence of c.863\_844insCGCT is the product of the relative incidences of GC (0.12), CG (0.17), GC (0.12), CT (0.08), and TG (0.28) extensions, corrected for the incidence of 5 nucleotide extensions (5.08%) and for unsuccessful events. These mutations require purine to pyrimidine switches (or vice versa) in 4/5 of the polymerizations (the maximum number of switches possible when starting and ending on a purine). Such switches are not favored by TdT because of its preference to stack nucleotides. The incidence of individual *NPM1* mutation 4-bp duplication/insertions at c.863 therefore varies over at least 4 orders of magnitude.

The second most common extension length is 2 nt. Only 2 such extensions are viable, TC and CC, with the second base providing occult microhomology. TC yields a type A mutation, CC a type D c.863\_864insCCTG. A total of 177 type D mutations were predicted; 160 were observed. There are 8 3-nt extension length mutations, all predicted at frequencies that should permit their detection here. All were observed, including the types A and D already discussed (TGTG: expected [exp] 9, observed [obs] 2; TATG: exp 11, obs 18; TTTG: exp 16, obs 2; TCTG: type A; CGTG: exp 6, obs 3; CATG: exp 9, obs 197; CTTG: exp 7, obs 32; and

CCTG: type D; supplemental Table 6). The exception among these concordant results was the CATG type B mutation, which was observed more frequently than expected (Figure 2). Other mutations with a CA root were not overrepresented, with the exception of CAGA. It is unclear why some CA root mutations are favored.

The model also predicts the incidence of individual mutations will fall as the number of nucleotide additions by TdT increases, partly because longer extensions are rarer but mainly because the overall number of potential mutations is increased with each extension. However, mutations with longer N-regions can occur more frequently than those with shorter N-regions if they are G/C rich and show significant nucleotide stacking. For example, c.863\_864insCCGG occurs more frequently than 3 of the 2-nt N-region mutations.

The calculations behind the model assume codon 289, coded entirely by the insertion, can accommodate any amino acid. Codon 289 represents the third amino acid in the L-xxx-V-xx-V-x-L NES, and a wide range of amino acids is clearly tolerated at this position (Tables 1 and 2). However, intolerance of some amino acids is suggested by the absence of certain predicted mutations (supplemental Table 6; Figure 2). Strikingly, none of the 8 4-bp insertions encoding p.Pro289 were observed (combined predicted incidence 49) (supplemental Tables 7 and 8),

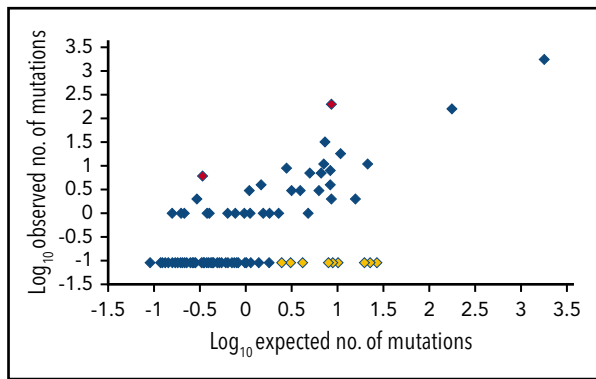


**Figure 2. Scatter plot of logarithmic transformations of observed vs predicted numbers of adult *NPM1* 4-bp insertion/duplication mutations at c.863\_864.**

From a cohort of 2257 independent mutations showing significant correlation between observed and predicted values. Each diamond represents 1 of the 122 possible mutations. Observed counts of 0 were substituted with the predicted occurrence of the rarest mutation to allow logarithmic transformation. Red diamonds: 2 most overrepresented mutations, c.863\_844insCATG and c.863\_844insCAGA. Yellow diamonds: 10 mutations predicted to occur 2 to 27 times in the cohort, but not observed.

suggesting intolerance of p.Pro289. Activity-based profiles of NESs predict reduced NES activity when proline is incorporated at position 3.<sup>26</sup> Our results suggest this reduced NES activity may impair creation of a functional *NPM1* mutation. Similarly, the 8 mutations encoding p.Gly289 were not observed (supplemental Table 7), although a single mutation encoding p.Gly289 was present in the pediatric cohort (Table 2). Glycine may therefore be poorly tolerated through creation of a weaker (but still functional) NES. Overall, a significant correlation was observed between the predicted and observed amino acid frequencies, even with inclusion of proline and glycine ( $\rho = 0.512$ ,  $P = .021$ ; Spearman rank correlation).

### Insertions at c.867\_868 and c.868\_869

The second most common insertion/indel position is c.867\_868, although still rare compared with c.863\_864 (1.28% vs 97.0%, Table 3). However, the number of mutations observed does not necessarily reflect the level of slippage/targeting of a particular site because only a fraction of mutations may be transforming and this fraction will vary from site to site. We applied the tenets of the TdT model to compare the levels of mutagenesis at these sites.

The c.867\_868 mutations consist of 4-bp insertions and longer indels (Tables 1 and 2). From the unrestrained *FLT3*-ITD data, we know that a majority (74%) of TdT extensions consist of 1 to 4 nucleotides, leading to *N*-regions of 1 to 3 nucleotides. However, all 4-nt insertions/duplications at c.867\_868 resulting from addition of 1 to 4 nucleotides to c.867G are predicted to lead to duplication of G in the 4th and final position of the insertion. This G, with the following TG, creates a GTG codon encoding valine at p.291, thereby breaking the W288 rule (the requirement to create a stronger NES when W288 is retained). The majority of slippage events at c.867\_868 will therefore not be observed.

However, if TdT adds  $\geq 5$  nucleotides to c.867G, then alternatives to p.Val291 become possible. The fifth nucleotide is used for occult microhomology, and these mutations therefore

appear as 4-bp insertions. There were 20 adult 4-bp pure insertions at c.867\_868, all with C, A, or T as the final nucleotide (Table 1). In comparison, there were 22 pure insertions at c.863\_864 (Table 5). This suggests at least equivalent levels of slippage at the 2 sites, whereas constraints on amino acid usage at p.290 (encoded entirely by the *N*-region) in c.867\_868ins(4) mutations suggests slippage at c.867\_868 may be higher than at c.863\_864.

### Pediatric vs adult mutations

*NPM1* mutations from children have a lower proportion of type A mutations than adults.<sup>5,6,16,17</sup> A key difference between type A and non-type A mutations is that type A mutations only require a single nucleotide addition by TdT, whereas the latter require 2 or more. The simplest explanation to account for the age-specific difference is therefore a higher level of TdT activity in pediatric myeloid stem cells. Increased TdT activity would bypass type A mutations in favor of those with longer extensions. We confirmed a significantly lower incidence of type A mutations in children (43/101 [42.6%], cf 1750/2322 [75.4%] in adults;  $P < .001$ , Fisher's exact test), then tested the predictions imposed by this solution.

First, *N*-regions should be longer on average in children than adults. Restricting analysis to mutations with visible *N*-nucleotides, the mean *N*-region in children was 3.80 nt ( $n = 55$ ), cf 2.46 nt in adults ( $n = 572$ ). Repeating the analysis with inclusion of all nonpoint mutations confirmed this finding; pediatric mean 2.11 nt ( $n = 99$ ), adult mean 0.61 nt ( $n = 2322$ ). However, these figures exclude the additional *N*-nucleotide required for occult microhomology. The mean numbers of total nucleotides added in children and adults are therefore 3.11 and 1.61, respectively, consistent with twofold higher TdT activity at younger age.

Second, this solution predicts differential use of insertion sites in adults and children. Insertions at c.867\_868 and c.868\_869 are longer than those at c.863\_864 in both adults and children (Tables 1 and 2). As discussed, replication errors at these alternative sites are predicted to occur more commonly than suggested by their observed incidence. With increased TdT activity, more *NPM1* insertions should reach the required length to use these alternative sites. Both of these sites are used at significantly increased frequency in children (ie, for c.867\_868 insertions,  $P = .008$ , Fisher's exact test) (Table 3).

Third, the model implies a different spectrum of c.863\_864ins(4) mutations in children. Although type A mutations occur at decreased frequency, changes in the frequency of the other c.863\_864ins(4) mutations should vary according to the number of TdT additions (2-5 nt) required for their genesis; the incidence of type D and type B mutations, requiring addition of 2 and 3 nucleotides, respectively, may not change equally. We categorized all c.863\_864ins(4) mutations by number of TdT nucleotide additions and compared the results between age groups (Table 5). Mutations requiring a single nucleotide are significantly underrepresented in children ( $P \leq .001$ , Fisher's exact test); those requiring 3 to 5 nucleotides are significantly overrepresented (31/83 [37.8%] in children, cf 347/2257 [15.4%] in adults;  $P \leq .001$  Fisher's exact test), whereas the incidence of 2 nucleotide extension mutations was not significantly changed (Table 5). In summary, the

**Table 5. *NPM1* c.863\_864 4 bp insertion/duplication mutations, according to their number of N-nucleotides**

No. N-nucleotides added	No. adult mutations observed (n = 2257)	Adult: % observed	Expected in population of n = 82	No. of pediatric mutations observed (n = 82)	Pediatric: ratio predicted/observed	P
1	1750	77.5	63.6	43	0.7	<.001
2	160	7.1	5.8	8	1.4	.379
3	254	11.3	9.2	22	2.4	<.001
4	71	3.1	2.6	7	2.7	.018
5	22	1.0	0.8	2	2.5	.205
3-5	347	15.4	12.6	31	2.5	<.001

A Bonferroni correction of 6 was applied, hence  $P < .0083$  was considered significant.

childhood incidences of type A, D, and B mutations are decreased, unchanged, and increased respectively. These results support the idea of differential TdT expression between adults and children, and the wider model that TdT drives *NPM1* mutagenesis.

## Discussion

In our accompanying paper, we suggest TdT plays a significant role in AML by priming replication slippage to generate *FLT3*-ITDs. Here we propose that *NPM1* mutations also arise following illegitimate TdT activity. Analysis of 2430 *NPM1* mutations confirms and extends the *FLT3*-ITD findings in an independent dataset using shared and complementary approaches. These findings propel TdT to membership of a select group of mutagenic lymphoid enzymes normally harnessed to promote antigenic diversity, but whose illegitimate activities promote cancer. These enzymes include RAG, which physiologically mediates V(D)J recombination at antigen receptor loci, but can cause oncogenic translocations in acute lymphoblastic leukemia and lymphoma<sup>27</sup>; and AID, a deaminating enzyme required for somatic hypermutation and class switch recombination that also induces off-target damage.<sup>28</sup> RAG, AID, and TdT therefore promote hematological neoplasia through distinct mutagenic activities. TdT is predicted to both prevent correct reintegration and promote mispriming during slippage.

We recognize that TdT is not expressed at high levels in *NPM1*-mutated AML at presentation and suggest that TdT levels may be down-regulated subsequent to mutation acquisition. There is a parallel for this in the presence of IG/TCR gene rearrangements in AML blasts that no longer retain expression of the RAG1/2 genes.<sup>29</sup>

The shared origin of *FLT3*-ITD and *NPM1* mutations explains their similar molecular anatomy. For both types of mutation, addition of nucleotides in excess of that required for priming results in visible G/C-rich N-regions, with significant nucleotide stacking, located between the 2 copies of the repeat. However, unlike *FLT3*-ITDs, *NPM1* mutations invariably require priming by TdT, reflecting a lack of appropriately positioned

germline microhomology. The marked cooccurrence between *NPM1* and *FLT3*-ITD mutations in AML<sup>2,5,6</sup> may in part be explained through this common origin, although these mutations are also recognized to show significant molecular synergy.<sup>19</sup>

The chance of creating a transforming *NPM1* mutation is defined through the dictates of a molecular roulette following addition of nucleotide(s) by TdT. There are only limited positions at which mispriming can occur that will lead to a transforming frameshift mutation, and such priming requires addition of the requisite complementary nucleotide. Choice of nucleotide is biased by TdT's G/C and stacking preferences, but each addition remains a chance event. Highly recurrent *NPM1* mutations reflect early addition of the correct N-nucleotide for appropriate priming. As the number of nucleotides added by TdT increases, the number of sequence permutations and possible mutations increases, and each mutation occurs at decreased frequency. The successful prediction of the incidence of the 4-bp 863\_864 *NPM1* insertions helps verify the TdT-mutator model. The success rate for creating functional *NPM1* mutations may be lower than for *FLT3*-ITDs because, although one-third of *FLT3* reintegrations will occur in frame through integration across a ~100-bp region, *NPM1* mutations may only have a single appropriate site. Elsewhere in AML genomes, indels occur only infrequently for reasons that remain unclear, but might reflect in part a need for a secondary structure (such as the *FLT3* palindrome) to facilitate access by TdT.

We also suggest why the *NPM1* mutation spectrum differs with age: a higher level of TdT activity in children may cause a shift away from type A mutations toward mutations with increasing number of N-nucleotides, including those at less commonly used insertion sites. TdT activity is known to vary with age.<sup>30-32</sup> This explains some of the genetic differences between adult and pediatric AML.<sup>33</sup>

In summary, the implication of TdT as a mutagen in AML is a significant finding, with key roles proposed in both *FLT3*-ITD and *NPM1* mutagenesis. Even allowing for the concurrence between these mutations, around one-half of all AML cases may arise following off-target TdT activity. Other AML mutations, such as *KIT*-ITDs, may also involve TdT. An increased incidence

of AML may therefore be part of the price we pay for adaptive immunity.

## Acknowledgment

The authors thank Joanne Mason (West Midlands Regional Genetics Laboratory) for critical reading of the manuscript.

## Authorship

Contribution: J.B. conceived the study, analyzed data, performed statistical analyses, and wrote the draft manuscript; S.A.D., S.A., and M.J.G. supervised the project; and all authors provided intellectual input, revised, and gave final approval to the manuscript.

Conflict-of-interest disclosure: The authors declare no competing financial interests.

ORCID profile: M.J.G., 0000-0001-5112-2882.

Correspondence: Julian Borrow, West Midlands Regional Genetics Laboratory, Birmingham Women's and Children's NHS Foundation Trust, Mindelsohn Way, Edgbaston, Birmingham, B15 2TG, United Kingdom; e-mail: j.borrow@nhs.net.

## Footnotes

Submitted 22 April 2019; accepted 30 September 2019. Prepublished online as *Blood* First Edition paper, 17 October 2019; DOI 10.1182/blood.2019001240.

The online version of this article contains a data supplement.

There is a *Blood* Commentary on this article in this issue.

The publication costs of this article were defrayed in part by page charge payment. Therefore, and solely to indicate this fact, this article is hereby marked "advertisement" in accordance with 18 USC section 1734.

## REFERENCES

- Grimwade D, Ivey A, Huntly BJP. Molecular landscape of acute myeloid leukemia in younger adults and its clinical relevance. *Blood*. 2016;127(1):29-41.
- Falini B, Mecucci C, Tiacci E, et al; GIMEMA Acute Leukemia Working Party. Cytoplasmic nucleophosmin in acute myelogenous leukemia with a normal karyotype. *N Engl J Med*. 2005;352(3):254-266.
- Arber DA, Orazi A, Hasserjian R, et al. The 2016 revision to the World Health Organization classification of myeloid neoplasms and acute leukemia. *Blood*. 2016;127(20):2391-2405.
- Haferlach C, Mecucci C, Schnittger S, et al. AML with mutated NPM1 carrying a normal or aberrant karyotype show overlapping biologic, pathologic, immunophenotypic, and prognostic features. *Blood*. 2009;114(14):3024-3032.
- Rau R, Brown P. Nucleophosmin (NPM1) mutations in adult and childhood acute myeloid leukaemia: towards definition of a new leukaemia entity. *Hematol Oncol*. 2009;27(4):171-181.
- Falini B, Nicoletti I, Martelli MF, Mecucci C. Acute myeloid leukemia carrying cytoplasmic/mutated nucleophosmin (NPMc+ AML): biologic and clinical features. *Blood*. 2007;109(3):874-885.
- Alcalay M, Tiacci E, Bergomas R, et al. Acute myeloid leukemia bearing cytoplasmic nucleophosmin (NPMc+ AML) shows a distinct gene expression profile characterized by up-regulation of genes involved in stem-cell maintenance. *Blood*. 2005;106(3):899-902.
- Mullighan CG, Kennedy A, Zhou X, et al. Pediatric acute myeloid leukemia with NPM1 mutations is characterized by a gene expression profile with dysregulated HOX gene expression distinct from MLL-rearranged leukemias. *Leukemia*. 2007;21(9):2000-2009.
- Schnittger S, Schoch C, Kern W, et al. Nucleophosmin gene mutations are predictors of favorable prognosis in acute myelogenous leukemia with a normal karyotype. *Blood*. 2005;106(12):3733-3739.
- Verhaak RGW, Goudswaard CS, van Putten W, et al. Mutations in nucleophosmin (NPM1) in acute myeloid leukemia (AML): association with other gene abnormalities and previously established gene expression signatures and their favorable prognostic significance. *Blood*. 2005;106(12):3747-3754.
- Nakagawa M, Kameoka Y, Suzuki R. Nucleophosmin in acute myelogenous leukemia. *N Engl J Med*. 2005;352(17):1819-1820, author reply 1819-1820.
- Nishimura Y, Ohkubo T, Furuichi Y, Umekawa H. Tryptophans 286 and 288 in the C-terminal region of protein B23.1 are important for its nucleolar localization. *Biosci Biotechnol Biochem*. 2002;66(10):2239-2242.
- Falini B, Bolli N, Shan J, et al. Both carboxy-terminus NES motif and mutated tryptophan(s) are crucial for aberrant nuclear export of nucleophosmin leukemic mutants in NPMc+ AML. *Blood*. 2006;107(11):4514-4523.
- Brunetti L, Gundry MC, Sorcini D, et al. Mutant NPM1 maintains the leukemic state through HOX expression. *Cancer Cell*. 2018;34(3):499-512.
- Brown P, McIntyre E, Rau R, et al. The incidence and clinical significance of nucleophosmin mutations in childhood AML. *Blood*. 2007;110(3):979-985.
- Brown P, Meshinchi S, Levis M, et al. Pediatric AML primary samples with FLT3/ITD mutations are preferentially killed by FLT3 inhibition. *Blood*. 2004;104(6):1841-1849.
- Thiede C, Creutzig E, Reinhardt D, Ehninger G, Creutzig U. Different types of NPM1 mutations in children and adults: evidence for an effect of patient age on the prevalence of the TCTG-tandem duplication in NPM1-exon 12. *Leukemia*. 2007;21(2):366-367.
- Borrow J, Dyer SA, Akiki S, Griffiths MJ. Terminal deoxynucleotidyl transferase promotes acute myeloid leukemia by priming FLT3-ITD replication slippage. *Blood*. 2019;134(25):2281-2290.
- Dovey OM, Cooper JL, Mupo A, et al. Molecular synergy underlies the co-occurrence patterns and phenotype of NPM1-mutant acute myeloid leukemia. *Blood*. 2017;130(17):1911-1922.
- Lieber MR. The mechanism of double-strand DNA break repair by the nonhomologous DNA end-joining pathway. *Annu Rev Biochem*. 2010;79(1):181-211.
- Messer PW, Arndt PF. The majority of recent short DNA insertions in the human genome are tandem duplications. *Mol Biol Evol*. 2007;24(5):1190-1197.
- Roth DB, Chang XB, Wilson JH. Comparison of filler DNA at immune, nonimmune, and oncogenic rearrangements suggests multiple mechanisms of formation. *Mol Cell Biol*. 1989;9(7):3049-3057.
- Bangs LA, Sanz IE, Teale JM. Comparison of D, JH, and junctional diversity in the fetal, adult, and aged B cell repertoires. *J Immunol*. 1991;146(6):1996-2004.
- Waanders E, Scheijen B, van der Meer LT, et al. The origin and nature of tightly clustered BTG1 deletions in precursor B-cell acute lymphoblastic leukemia support a model of multiclonal evolution. *PLoS Genet*. 2012;8(2):e1002533.
- Gauss GH, Lieber MR. Mechanistic constraints on diversity in human V(D)J recombination. *Mol Cell Biol*. 1996;16(1):258-269.
- Kosugi S, Yanagawa H, Terauchi R, Tabata S. NESmapper: accurate prediction of leucine-rich nuclear export signals using activity-based profiles. *PLOS Comput Biol*. 2014;10(9):e1003841.
- Marculescu R, Vanura K, Montpellier B, et al. Recombinase, chromosomal translocations and lymphoid neoplasia: targeting mistakes and repair failures. *DNA Repair (Amst)*. 2006;5(9-10):1246-1258.
- Rebhandl S, Huemer M, Greil R, Geisberger R. AID/APOBEC deaminases and cancer. *Oncoscience*. 2015;2(4):320-333.
- Boeckx N, Willems MJ, Szczepanski T, et al. Fusion gene transcripts and Ig/TCR gene

- rearrangements are complementary but infrequent targets for PCR-based detection of minimal residual disease in acute myeloid leukemia. *Leukemia*. 2002;16(3): 368-375.
30. Murray JM, O'Neill JP, Messier T, et al. V(D)J recombinase-mediated processing of coding junctions at cryptic recombination signal sequences in peripheral T cells during human development. *J Immunol*. 2006;177(8): 5393-5404.
31. Schneider M, Panzer S, Stolz F, Fischer S, Gadner H, Panzer-Grümayer ER. Crosslineage TCR delta rearrangements occur shortly after the DJ joinings of the IgH genes in childhood precursor B ALL and display age-specific characteristics. *Br J Haematol*. 1997;99(1): 115-121.
32. Champagne DP, Shockett PE. Illegitimate V(D)J recombination-mediated deletions in Notch1 and Bcl11b are not sufficient for extensive clonal expansion and show minimal age or sex bias in frequency or junctional processing. *Mutat Res*. 2014;761: 34-48.
33. Creutzig U, van den Heuvel-Eibrink MM, Gibson B, et al; AML Committee of the International BFM Study Group. Diagnosis and management of acute myeloid leukemia in children and adolescents: recommendations from an international expert panel. *Blood*. 2012;120(16): 3187-3205.